

Accepted Article

Title: Dynamic Evolution of Aluminum Coordination Environments in Mordenite Zeolite and Their Role in the Dimethyl Ether (DME) Carbonylation Reaction

Authors: Rongsheng Liu, Benhan Fan, Yuchun Zhi, Chong Liu, Shutao Xu, Zhengxi Yu, and Zhongmin Liu

This manuscript has been accepted after peer review and appears as an Accepted Article online prior to editing, proofing, and formal publication of the final Version of Record (VoR). The VoR will be published online in Early View as soon as possible and may be different to this Accepted Article as a result of editing. Readers should obtain the VoR from the journal website shown below when it is published to ensure accuracy of information. The authors are responsible for the content of this Accepted Article.

To be cited as: *Angew. Chem. Int. Ed.* **2022**, e202210658

Link to VoR: <https://doi.org/10.1002/anie.202210658>

RESEARCH ARTICLE

Dynamic Evolution of Aluminum Coordination Environments in Mordenite Zeolite and Their Role in the Dimethyl Ether (DME) Carbonylation Reaction

Rongsheng Liu,^{[a], [b]} Benhan Fan,^{[a], [b]} Yuchun Zhi,^[a] Chong Liu,^{[a], [b]} Shutao Xu,^[a] Zhengxi Yu,^{*[a]} and Zhongmin Liu^{*[a], [b]}

[a] R. Liu, B. Fan, Y. Zhi, C. Liu, S. Xu, Z. Yu, Z. Liu
National Engineering Research Center of Lower-Carbon Catalysis Technology, Dalian National Laboratory for Clean Energy
Dalian Institute of Chemical Physics, Chinese Academy of Sciences
Dalian 116023, China
E-mail: zhengxiyu@dicp.ac.cn; liuzm@dicp.ac.cn

[b] R. Liu, B. Fan, C. Liu, Z. Liu
University of Chinese Academy of Sciences
Beijing 100049, China

Supporting information for this article is given via a link at the end of the document.

Abstract: Part of tetrahedral framework aluminum in a protonic mordenite (HMOR) will convert geometry to distorted tetrahedral and octahedral coordination. High-field ^{27}Al NMR data show that more framework Al atoms at T_3 and T_4 sites change geometry to nonframework structures than others. These nonframework Al species preferentially reside in the side pockets, which will decrease the accessibility of acid sites in the 8-membered ring (MR) channel, impairing the dimethyl ether (DME) carbonylation reaction. The arisen octahedrally coordinated Al species are framework-associated, which can be reverted into the zeolite framework. Herein, we find that a facile treatment with pyridine could force the octahedral coordination Al back into a tetrahedral environment, which could increase the number of available active sites and enhance the diffusion of DME, thus improving the reactivity (4 times) of the DME carbonylation reaction and prolonging the lifetime of catalysts.

Introduction

Zeolites have played indispensable roles in many chemical synthesis and petrochemical processes for decades, owing to their variable microporous framework structures and acidities. The demanding economic and environmental requirements motivate the persisting exploration on the zeolite structure-performance relationship and the rational design of catalyst.^[1] One prominent feature of zeolitic acidic properties is embodied by the Brønsted acid sites (BASs), appearing as protons (one kind of the extra-framework cations) to balance the negative charges of $[\text{AlO}_4]^-$ units in aluminosilicate zeolites.^[2] Besides, certain Al species appearing in nonframework structures of zeolites function as the Lewis acid sites (LASs), which are essential for catalysis reactions such as cracking and biomass conversion reactions.^[3] Therefore, a prerequisite for understanding the zeolite structure-performance relationship is to discern the distribution and location of Al species in the zeolite framework and nonframework structures.^[4] Conventionally, solid-state ^{27}Al MAS (magic-angle spinning) NMR is sensitive to the coordination environment of Al

species in the zeolite and is usually employed to study the location of Al atoms in framework and nonframework sites.^[5]

Mordenite (MOR) zeolite, consisting of parallel 12- and 8-membered ring (MR) channels (7.0×6.5 and 5.7×2.6 Å) connected by 8-MR side pockets (4.8×3.4 Å) (Figure S1), exhibits exceptional catalytic performance for the carbonylation of dimethyl ether (DME), due to its unique 8-MR pore structure.^[6] The BASs associated with the crystallographically T_3 (tetrahedra) sites within the 8-MR channel have been identified as the most active acid sites.^[7] Moreover, the 12-MR main channel provides a transport channel for the reactions, and the BASs in the 12-MR channel will result in rapid deactivation of the MOR catalyst.^[8] Recently, our groups successfully realized the directional migration of Al from 12-MR to 8-MR by a low-pressure SiCl_4 treatment, which noticeably enhances the carbonylation reactivity and elongates the catalyst lifetime.^[9] This progress provides a facile strategy for controllable redistribution of BASs and enriches our understanding of the structure-performance relationship exerted by the unique topological structure of the 8-MR channel. However, LASs properties, including the spatial distributions and chemical transformations and their correlations with the carbonylation performance, are not well elaborated.

Steaming, chemical leaching, and calcination at high temperature are the frequently adopted approaches to modulate Al coordination from tetrahedral framework structure to octahedral nonframework structure.^[10] These post-treatments result in the Si-O-Al bonds hydrolyzing, thus extracting Al atoms from the zeolite framework.^[11] Multitudinous Al species in nonframework structures, such as $\text{Al}(\text{OH})_3$, AlOOH , $\text{Al}(\text{OH})^{2+}$, Al_2O_3 , and multinuclear clusters (which usually adopt three-, penta-, and hexa-coordination), were detected.^[12] The distorted tetrahedral coordination Al species also commonly appear in zeolites, broadening the ^{27}Al NMR peak shape of framework Al species.^[13] Besides, some kinds of Al species that are partially dislodged from the zeolite framework (referred to as framework-associated aluminum) were also probed, and they could undergo reversible modulation between octahedral and tetrahedral coordination.^[10e, 14] Ravi. et al. testified that framework-associated aluminum was associated with LASs in MOR zeolite by combining FTIR and ^{27}Al

RESEARCH ARTICLE

MAS NMR technologies.^[15] Moreover, such octahedrally coordinated Al species can be forced back into the framework to restore the tetrahedral coordination.^[14, 16] The octahedrally coordinated Al is the precursor of LASs, and its formation is accompanied by a loss in BASs, and such LASs have a preferred location in the side pockets of MOR zeolite.^[3a] Some T-sites are more prone to generate framework-associated aluminum than other positions in zeolites.^[16a] These nonframework Al species give rise to Lewis acidity and bring out the synergy between Brønsted and Lewis acid sites, which can enhance the catalytic versatility of zeolites.^[16b, 17] However, the diffusion of molecules into zeolite crystals may be restricted to a certain extent if the channels are blocked by the nonframework Al species.^[18] Even though these progresses, the dynamic evolution of Al coordination environments in distinct 8-MR and 12-MR topological spaces and the influence of coordination alteration on the carbonylation performance are still less understood. This work aims to further understand the character of these Al species in nonframework structure and to control the formation of such Al species to improve the catalytic performance.

In this work, we proposed that more framework Al atoms at T₃ and T₄ sites are converted into octahedral and distorted tetrahedral coordination than other positions, and the amount of nonframework Al species is linearly correlated with the calcination temperature of NH₄-MOR (ammonium form MOR zeolite). Such

nonframework Al species are preferentially located in the side pockets of MOR zeolite, which will block DME reactants from accessing the catalytically active acid sites within the 8-MR channel, reducing the reactivity of the DME carbonylation reaction. Adsorption of pyridine is an effective method to make the octahedrally coordinated Al species revert into typical tetrahedral coordination, thereby improving the catalytic performance due to the increase of the reactively favorable framework Al atoms and the diffusion ability of DME into the 8-MR environment.

Results and Discussion

Conventionally, the aluminum coordination in protonic MOR (HMOR) zeolite is recognized by ²⁷Al MAS and MQMAS (multiple-quantum magic-angle spinning) NMR spectroscopy. Before testing, the samples are fully hydrated at room temperature to restrain the large quadrupolar interaction. The effect of the hydrated counteraction on the ²⁷Al isotropic chemical shift is negligible^[4, 5c, 19], which was validated by the roughly overlapping of the ²⁷Al MAS NMR spectra of Na-MOR and NH₄-MOR samples (Figure S2). Therefore, the obtained ²⁷Al chemical shifts for MOR samples with different hydrated counteractions can be comparable.

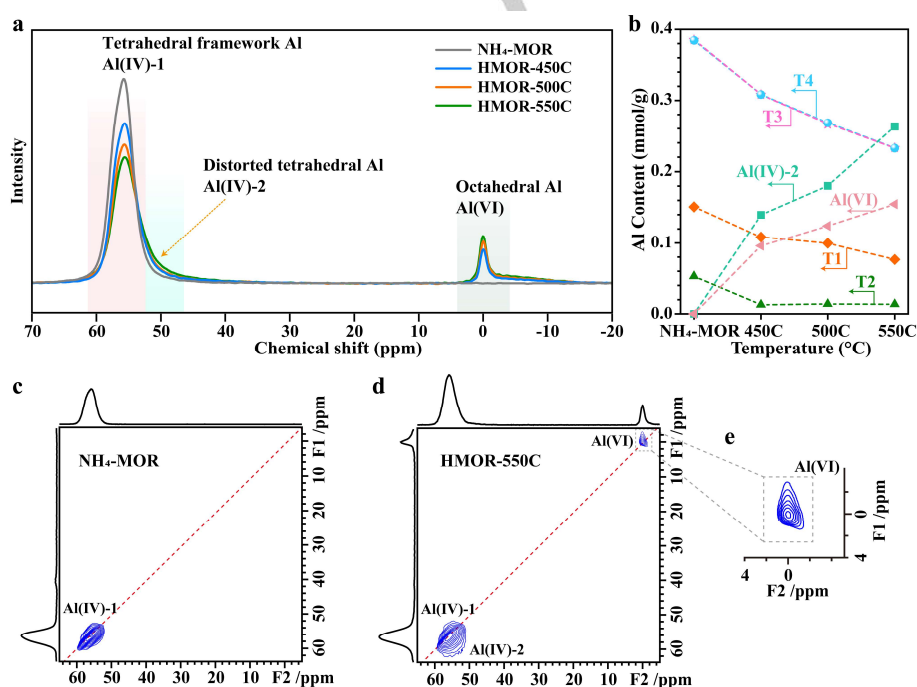


Figure 1. a) ²⁷Al MAS NMR spectra of varying MOR samples acquired at 18.8 T. b) The evolution of different Al species in framework and nonframework structures with increasing calcination temperature and the data obtained from a combination of ²⁷Al MAS NMR and XRF. ²⁷Al MQMAS NMR spectra measured for (c) NH₄-MOR and (d) HMOR-550C. Enlargement of the Al(VI) signal region in (d) is shown in (e).

Figure 1 summarizes the ²⁷Al NMR spectra acquired at 18.8 T for a series of MOR samples. The spectrum of NH₄-MOR only shows a resonance peak at ~56 ppm, indicating that almost all Al species adopt framework tetrahedral coordination.^[9, 13a] After calcining NH₄-MOR at different temperatures (450–550 °C), part of the framework tetrahedral Al species are changed into octahedral coordination, evidenced by the presence of sharp 0 ppm resonance (Figure 1a).^[17b] Meanwhile, the framework Al

signal at ~56 ppm of HMOR samples shows a broad shoulder resonance extending to the upfield. This broadening, not discernible in the spectrum of NH₄-MOR, might be associated with the distorted tetrahedral Al atoms (40–50 ppm region) (Figure 1a).^[5a, 13b, 17b] The change in the coordination environment of Al species was further examined by the ²⁷Al MQMAS NMR spectra. The spectrum of NH₄-MOR shows a single feature labeled Al(IV)-1 with a low anisotropic quadrupolar interaction (Figure 1c),

RESEARCH ARTICLE

assigned to tetrahedrally coordinated framework Al.^[4, 20] Besides the presence of Al(IV)-1 site, the Al(IV)-2 signal with the significant quadrupolar effect reflected in the broad contours parallel to the F2 dimension appears in the HMOR-550C sample in Figure 1d, in agreement with the broadening in Figure 1a, which can be assigned to the distorted tetrahedral Al species.^[3a] It is clear that there are four framework Al sites in MOR zeolite, and by now, the chemical shift and unique quadrupolar parameters of these Al species of MOR zeolite can be obtained.^[9] Likewise, these parameters of distorted tetrahedral Al can also be obtained from the known methods for shearing (Figure S3 and Table S2). Figure 1e also shows at least two types of Al(VI) sites (octahedrally coordinated Al species) in the HMOR-550C sample, but additional work is required to confirm such an assignment.

Figure 1a shows that the type of Al species in MOR zeolite is a function of the counteraction and calcination temperature^[3a, 21], and the change in the relative amount of different Al species indicates that the tetrahedrally coordinated framework Al increasingly converts geometry to octahedral and distorted tetrahedral coordination with increasing calcination temperature. Moreover, a combination of XRF and the deconvolution of ²⁷Al NMR are used to quantify the Al species in each framework T-sites and nonframework structures (Figure S4 and Table S3). Figure 1b shows that with the increase of calcination temperature, the amount of framework Al atoms at all four T-sites decreases, and the order of framework Al atoms which are more prone to be converted into nonframework structure is that: T₂ > T₁ > T₃ = T₄, consistent with site energy of the different T-sites obtained from simulation results.^[22] However, more Al atoms at T₃ and T₄ sites change geometry to octahedral and distorted tetrahedral coordination than others, owing to most framework Al atoms (ca. 75-80 %) occupancy at T₃ + T₄ sites.^[9, 23] Furthermore, the change in the coordination and content of Al species would affect the type and number of hydroxyl groups in zeolite. Figure S5 shows the ¹H MAS NMR spectra for varying HMOR samples corresponding to Figure 1. Three well-known signals at approximately 4.0, 2.5, and 1.8 ppm are assigned to the acidic bridging hydroxyl (BASs), certain Al hydroxyl (Al-OH), and nonacidic silanol hydroxyl (Si-OH) groups, respectively.^[8b] The gradual decrease of BASs is accompanied by a relevant increase of Al-OH with increasing calcination temperature, which is in agreement with the variation trend of Al species, as shown in Figure 1.

To study the characteristic of Al species in nonframework structures, HMOR zeolites were treated with different methods. Figure 2 shows the ²⁷Al NMR spectra acquired at 18.8 T for varying HMOR-550C samples with different treatments. As mentioned above, the term 'framework-associated aluminum' referred to the octahedrally coordinated Al species that are not entirely removed from the zeolite framework, which have a memory of their native position and could be forced back into tetrahedral coordination.^[10e] Figure 2a shows that the resonance at 0 ppm vanished with the isochronous increase in the signal at ~56 ppm when the HMOR-550C sample was exchanged back into the ammonium form, thereby indicating that these octahedral coordination Al species are 'framework-associated'. Meanwhile, part of distorted tetrahedral coordination Al species is also converted into framework tetrahedral, evidenced by the weakening of the shoulder resonance at 40~50 ppm. As was noted with the ²⁷Al MQMAS NMR spectrum in Figure 2b, the signal corresponding to Al(VI) sites disappears, while some

Al(IV)-2 feature is reserved during the ammonium exchange process.

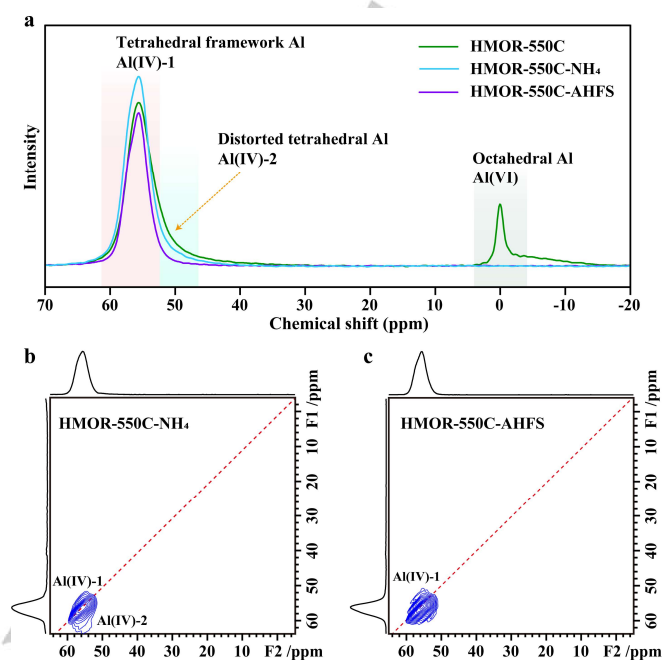


Figure 2. a) ²⁷Al MAS NMR spectra of the HMOR-550C sample with different treatments at 18.8 T magnetic field strengths. ²⁷Al MQMAS NMR spectra measured for (b) HMOR-550C-NH₄ and (c) HMOR-550C-AHFS.

The nonframework Al species can be selectively removed without damaging the framework structure by ammonium hexafluorosilicate (AHFS) under mild treatment.^[4, 24] Herein, some HMOR-550C samples were treated with AHFS under appropriate conditions, denoted as HMOR-550C-AHFS, to trace the location of nonframework Al species. From Figure 2a, the overall Al species in the HMOR-550C decreased obviously after treating with AHFS. Notably, the octahedral and distorted tetrahedral coordination Al species are not detectable. The signals corresponding to Al(IV)-2 and Al(VI) sites disappear in Figure 2c, revealing that the nonframework Al species have been removed through AHFS treatment. XRF analysis shows that the Si/Al ratio increases from 16.1 for the HMOR-550C to 29.1 for the HMOR-550C-AHFS (Table S1). The removed proportion of Al (41 %) agrees with the content of nonframework Al species (42 %), thus indicating the selective removal of nonframework tetrahedral Al species. Despite the removal of Al species by AHFS treatment, the number of acid sites probed by NH₃-TPD increased significantly (Figure S6). In contrast, the N₂ physisorption results suggest no significant changes occurred in the pore structure after treating with AHFS (Figure S7 and Table S1). These measured data could not explore whether the increase of acid sites is concerned with framework Al or nonframework Al species.

To answer this question, we investigate the diffusion behaviors of *n*-hexane and DME molecules in HMOR zeolites by performing uptake measurements in an intelligent gravimetric analyzer (IGA). The long-chain *n*-hexane molecule with a diameter of around 0.43 nm can selectively enter the 12-MR channel instead of the 8-MR channel of MOR zeolite^[18, 25], while the molecular diameter of DME is small enough to visit both 12- and 8-MR channels.^[8a, 26] The results for the uptake of probe molecules are shown in Figure

RESEARCH ARTICLE

3. The similar equilibrium uptakes of *n*-hexane by the HMOR-550C and HMOR-550C-AHFS samples (Figure 3a) indicate the comparable availability of the 12-MR channel for the two samples. In contrast, the adsorption of DME on two samples is quite different, as shown in Figure 3b. About 55 % increase in the DME equilibrium uptake at 20 bar for the HMOR-550C-AHFS relative to the HMOR-550C sample, suggesting the significant increase of availability of the micropore volume after removing the nonframework Al species. The above results show that the uptake of DME is highly related to the presence of nonframework Al species that block the DME molecules from diffusing into the 8-MR channel, while the uptake of *n*-hexane is almost unaffected by the presence of nonframework Al species. In addition, reactants and products enter the 8-MR channel of MOR zeolite through the side pockets only.^[8a, 8b] This allows us to infer that most of the nonframework Al species reside in the side pockets, which will reduce the availability of acid sites within the 8-MR channel.

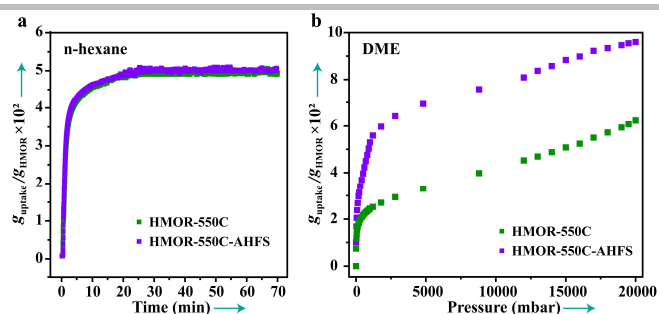


Figure 3. a) Experimental uptake curves for *n*-hexane over HMOR-550C and HMOR-550C-AHFS at 323 K and a total pressure of 300 mbar. b) DME adsorption isotherms of the HMOR-550C and HMOR-550C-AHFS at 323 K.

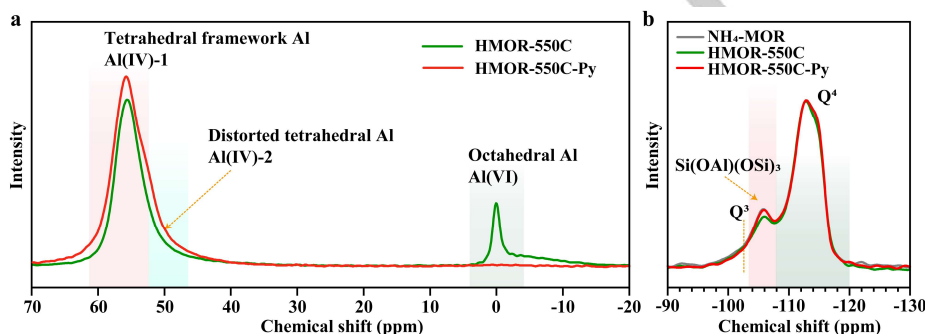


Figure 4. a) ²⁷Al MAS NMR spectra of the HMOR-550C and HMOR-550C-Py (Pyridine) samples at 18.8 T. b) ²⁹Si MAS NMR spectra of NH₄-MOR, HMOR-550C, and HMOR-550C-Py.

Figure 4a shows the ²⁷Al NMR spectrum of the HMOR-550C-Py sample (pre-adsorption of pyridine). From this data, the resonance at 0 ppm corresponding to octahedrally coordinated Al species disappears without affecting the Si/Al ratio (Table S1), indicating that the framework-associated Al can also be reverted into the tetrahedral environment upon adsorbing pyridine. However, it is difficult to give more detailed information on the change of Al species in the framework, owing to the broadening of framework Al signals, which may be caused by the pyridine-modified chemical environments and the impeded hydration by pyridine present in the channel.^[4, 5c] Thus, we chose ²⁹Si MAS NMR to analyze the variation trend of the number of framework Al species of HMOR-550C samples before and after pyridine adsorption (Figure 4b). In the ²⁹Si NMR, the primary signals at -110 ~ -116 ppm can be ascribed to Q⁴, Si(OSi)₄, species, and the resonances at about -106 and -103 ppm are assigned to Si(OAl)(OSi)₃ and Q³ Si(OH)(OSi)₃ species, respectively.^[27] The quantitative results were obtained from the deconvolution of ²⁹Si NMR spectra. There is about a 12 % decrease in the resonance signal area at -106 ppm corresponding to Si(1Al)(OSi)₃ species for the HMOR-550C sample relative to the NH₄-MOR. Upon adsorption of pyridine on HMOR-550C, the loss of total signal area is almost entirely restored, due to the reversion of Si-O-Al bonds, verifying that pyridine treatment can reverse framework-associated Al into tetrahedral framework coordination.

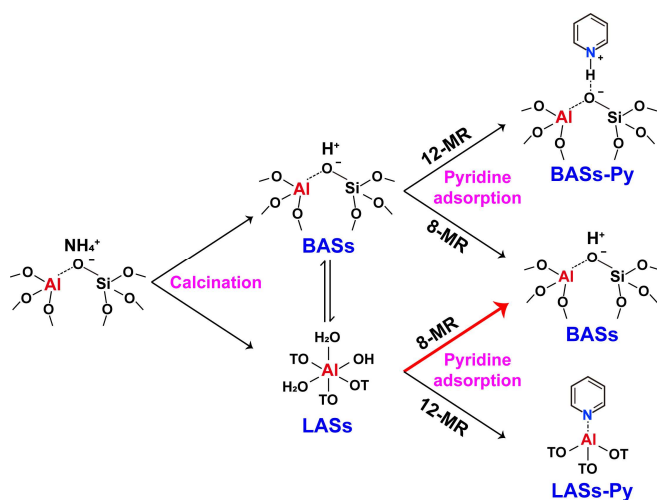
It is well-known that pyridine is usually used to probe the acid sites in the 12-MR channel of HMOR zeolite, owing to the restriction of its molecular size.^[6a, 28] Hence, it should be

separately discussed that the reason why pyridine reverts nonframework Al species into framework coordination. For the 12-MR channel, pyridine easily approaches the nonframework Al species, forming the LASs-Py, evidenced by the signal at 1450 cm⁻¹ in Py-FTIR (Figure S8), which converts these nonframework Al species into tetracoordination.^[3b] For the 8-MR channel, despite pyridine hardly accessing this environment through side pockets, we also observed the interaction between acidic hydroxyls within the 8-MR channel and pyridine.^[28] Likewise, we think the pyridine, which might be adsorbed in the pore mouth of side pockets, will interact with the nonframework Al species in the 8-MR channel, thereby forcing them back into the zeolite framework, reflected in the entire reversion of Si-O-Al bonds in ²⁹Si MAS NMR. This driving force might be caused by the additional steric-hindrance effect, the change of electric field, or structure-directing of pyridine after adsorbing pyridine.^[1a, 29]

The dynamic evolution of aluminum coordination environments in MOR zeolite along with treatment conditions were illustrated in Scheme 1. All Al species adopt tetrahedral framework coordination in the NH₄-MOR sample. NH₄-MOR transforms into proton form after calcination leading to the formation of BASs. Meanwhile, part of the framework tetrahedral Al is changed geometry into the octahedral coordination, which is demonstrated as framework-associated Al, yielding LASs. Upon pyridine adsorption, different Al species in distinct 8-MR and 12-MR topological spaces occur complex interactions with pyridine. In the 12-MR channel, the pyridine molecule bonds with BASs, forming BASs-Py, thereby poisoning the acid sites. Moreover,

RESEARCH ARTICLE

pyridine acts on the octahedral coordination Al species, causing the LASs-Py species, which converts the nonframework Al species into tetracoordination, consistent with the previous report by Christophe Copéret.^[3b] In the case of the 8-MR channel, the adsorption and desorption behaviors of pyridine on the BASs within the 8-MR channel were observed.^[28] There is no effect on the BASs within 8-MR channels by pyridine in this pyridine adsorption condition. In contrast, adsorbed pyridine forces the octahedral coordination Al species in the 8-MR back into the zeolite framework, thus yielding more BASs in the 8-MR channel. As such, pyridine adsorption is helpful in obtaining a MOR catalyst with more framework Al atoms in the 8-MR channel, and the acid sites in the 12-MR channel are deactivated.



Scheme 1. Sketch map of the dynamic evolution of aluminum coordination environments in mordenite zeolite and its influence on acid sites.

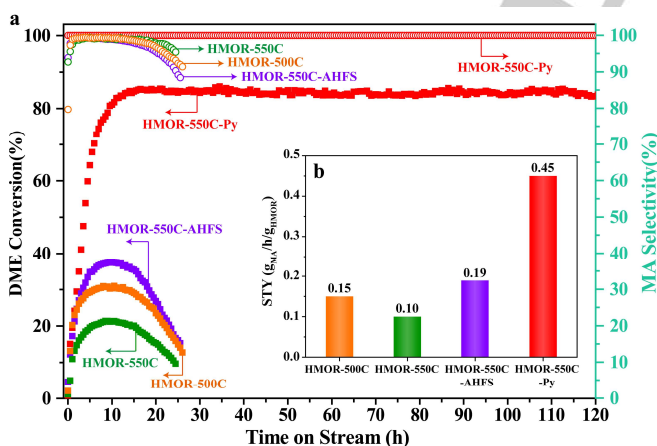


Figure 5. a) DME conversion, MA selectivity, and (b) MA space-time yield (STY) over HMOR catalysts with different preparations on the DME carbonylation to MA reaction. Reaction conditions: 200 °C, 2 Mpa, DME/CO/H₂=5/35/60, GHSV=3120 ml·g⁻¹·h⁻¹.

Figure 5a shows the remarkably different reactivity of DME carbonylation on varying HMOR samples. The DME conversion decreased with the increasing calcination temperature, due to more removal of framework Al from the T₃ site, and a decrease in the availability of acid sites within the 8-MR channel caused by

nonframework Al species. Upon treating the HMOR-550C sample with AHFS, the DME conversion increased significantly, owing to the removal of nonframework Al species that remarkably improves the availability of acid sites.

Pyridine adsorption, the most effective method to selectively poison acid sites within the 12-MR channels that are responsible for coke formation and deactivation of MOR catalyst, prolongs the lifetime for the DME carbonylation to methyl acetate (MA) reaction that is the key step in DME-to-ethanol (DMTE) process.^[28, 30] Figure 5 shows the remarkably longer catalytic lifetime of 120 h for the pre-adsorption pyridine sample labeled as HMOR-550C-Py, without deactivation during the catalytic evaluation period, than that of other samples (about 10 h) without pyridine adsorption. Another striking observation is that the DME conversion on the HMOR-550C sample after adsorption of pyridine was significantly increased by a factor of 4, and the space-time yield (STY) of MA increased from 0.10 g_{MA}/h/g_{HMOR} for HMOR-550C to 0.45 g_{MA}/h/g_{HMOR} for HMOR-550C-Py (Figure 5b), because the nonframework Al species are forced back into the tetrahedral environment. This change could increase the number of Al atoms in the T₃ site and improve the availability of acid sites within the 8-MR channel. Thereby, pre-adsorption of pyridine not only significantly elongates the lifetime of HMOR zeolite but also remarkably improves the MA STY, which holds the potential to upgrade the commercial DMTE process.

Conclusion

Protonic mordenite (HMOR) zeolite, obtained by calcining the ammonium form MOR (NH₄-MOR) zeolite, is the important catalyst for the DME carbonylation reaction. During calcining the NH₄-MOR at high temperatures, a fraction of framework Al atoms change geometry into distorted tetrahedral and octahedral coordination. Therein, the octahedral coordination Al is framework-associated, which could be reverted into the zeolite framework. The loss of framework Al atoms mainly occurs in the T₄ and T₃ sites of HMOR, the latter site being the most active site for the DME carbonylation reaction. These nonframework Al species preferentially reside in the side pockets, which is unfavorable for DME molecules to access acid sites within the 8-MR channel, weakening the catalytic performance of the DME carbonylation reaction. Pre-absorption of pyridine could force the framework-associated Al species back into a tetrahedral environment, which can increase the number of Al atoms in the T₃ site and improve the availability of acid sites within the 8-MR channel, thereby enhancing the DME conversion and prolonging the lifetime of HMOR zeolite.

Acknowledgements

This work was supported by the National Natural Science Foundation of China (Nos. 21991090, 21991093).

Conflict of interest

The authors declare no conflict of interest.

RESEARCH ARTICLE

Keywords: zeolite • aluminum coordination • heterogeneous catalysis • DME carbonylation • pyridine

- [1] a) Y. Chai, W. Dai, G. Wu, N. Guan, L. Li, *Acc. Chem. Res.* **2021**, *54*, 2894-2904; b) W. O. Haag, R. M. Lago, P. B. Weisz, *Nature* **1984**, *309*, 589-591.
- [2] a) A. Corma, *Chem. Rev.* **1995**, *95*, 559-614; b) C. G. Li, A. Vidal-Moya, P. J. Miguel, J. Dedecek, M. Boronat, A. Corma, *ACS Catal.* **2018**, *8*, 7688-7697.
- [3] a) M. Ravi, V. L. Sushkevich, J. A. van Bokhoven, *Chem. Sci.* **2021**, *12*, 4094-4103; b) A. V. Yakimov, M. Ravi, R. Verel, V. L. Sushkevich, J. A. van Bokhoven, C. Copéret, *J. Am. Chem. Soc.* **2022**, *144*, 10377-10385; c) H. Y. Luo, J. D. Lewis, Y. Roman-Leshkov, in *Annual Review of Chemical and Biomolecular Engineering, Vol 7, Vol. 7* (Ed.: J. M. Prausnitz), **2016**, pp. 663-692.
- [4] K. Z. Chen, Z. H. Gan, S. Horstmeier, J. L. White, *J. Am. Chem. Soc.* **2021**, *143*, 6669-6680.
- [5] a) K. Chen, S. Horstmeier, V. T. Nguyen, B. Wang, S. P. Crossley, T. Pham, Z. Gan, I. Hung, J. L. White, *J. Am. Chem. Soc.* **2020**, *142*, 7514-7523; b) A. Vjunov, J. L. Fulton, T. Huthwelker, S. Pin, D. Mei, G. K. Schenter, N. Govind, D. M. Camaioni, J. Z. Hu, J. A. Lercher, *J. Am. Chem. Soc.* **2014**, *136*, 8296-8306; c) S. Sklenak, J. Dedecek, C. B. Li, B. Wichterlova, V. Gabova, M. Sierka, J. Sauer, *Angew. Chem. Int. Ed.* **2007**, *46*, 7286-7289; d) S. Sklenak, J. Dedecek, C. Li, B. Wichterlova, V. Gabova, M. Sierka, J. Sauer, *Phys. Chem. Chem. Phys.* **2009**, *11*, 1237-1247.
- [6] a) R. Liu, S. Zeng, T. Sun, S. Xu, Z. Yu, Y. Wei, Z. Liu, *ACS Catal.* **2022**, *12*, 4491-4500; b) X. Yi, Y. Xiao, G. Li, Z. Liu, W. Chen, S.-B. Liu, A. Zheng, *Chem. Mater.* **2020**, *32*, 1332-1342; c) K. Gong, Z. Liu, L. Liang, Z. Zhao, M. Guo, X. Liu, X. Han, X. Bao, G. Hou, *J. Phys. Chem. Lett.* **2021**, *12*, 2413-2422; d) W. Chen, G. C. Li, X. F. Yi, S. J. Day, K. A. Tarach, Z. Q. Liu, S. B. Liu, S. C. E. Tsang, K. Gora-Marek, A. M. Zheng, *J. Am. Chem. Soc.* **2021**, *143*, 15440-15452; e) Y. Li, S. Y. Huang, Z. Z. Cheng, K. Cai, L. D. Li, E. Milan, J. Lv, Y. Wang, Q. Sun, X. B. Ma, *Appl. Catal. B* **2019**, *256*, 12.
- [7] a) A. Bhan, A. D. Allian, G. J. Sunley, D. J. Law, E. Iglesia, *J. Am. Chem. Soc.* **2007**, *129*, 4919-4924; b) M. Boronat, C. Martinez-Sanchez, D. Law, A. Corma, *J. Am. Chem. Soc.* **2008**, *130*, 16316-16323; c) P. Cheung, A. Bhan, G. Sunley, D. Law, E. Iglesia, *J. Catal.* **2007**, *245*, 110-123.
- [8] a) Z. Q. Liu, X. F. Yi, G. R. Wang, X. M. Tang, G. C. Li, L. Huang, A. M. Zheng, *J. Catal.* **2019**, *369*, 335-344; b) T. He, X. C. Liu, S. T. Xu, X. W. Han, X. L. Pan, G. J. Hou, X. H. Bao, *J. Phys. Chem. C* **2016**, *120*, 22526-22531; c) Z. Z. Cheng, S. Y. Huang, Y. Li, J. Lv, K. Cai, X. B. Ma, *Ind. Eng. Chem. Res.* **2017**, *56*, 13618-13627.
- [9] R. S. Liu, B. H. Fan, W. N. Zhang, L. Y. Wang, L. Qi, Y. L. Wang, S. T. Xu, Z. X. Yu, Y. X. Wei, Z. M. Liu, *Angew. Chem. Int. Ed.* **2022**, *134*, e202116990.
- [10] a) R. A. Beyerlein, C. Choi-Feng, J. B. Hall, B. J. Huggins, G. J. Ray, *Top. Catal.* **1997**, *4*, 27-42; b) A. W. Odonovan, C. T. Oconnor, K. R. Koch, *Microporous Mater.* **1995**, *5*, 185-202; c) G. H. Kuehl, H. K. C. Timken, *Microporous Mesoporous Mater.* **2000**, *35-6*, 521-532; d) M. C. Silaghi, C. Chizallet, J. Sauer, P. Raybaud, *J. Catal.* **2016**, *339*, 242-255; e) M. Ravi, V. L. Sushkevich, J. A. van Bokhoven, *Nat. Mater.* **2020**, *19*, 1047-1056.
- [11] a) L. D. Fernandes, P. E. Bartl, J. L. F. Monteiro, J. G. o. da Silva, S. n. C. de Menezes, M. J. B. Cardoso, *Zeolites* **1994**, *14*, 533-540; b) X. Yi, K. Liu, W. Chen, J. Li, S. Xu, C. Li, Y. Xiao, H. Liu, X. Guo, S.-B. Liu, A. Zheng, *J. Am. Chem. Soc.* **2018**, *140*, 10764-10774.
- [12] a) S. Li, A. Zheng, Y. Su, H. Zhang, L. Chen, J. Yang, C. Ye, F. Deng, *J. Am. Chem. Soc.* **2007**, *129*, 11161-11171; b) R. D. Shannon, K. H. Gardner, R. H. Staley, G. Bergeret, P. Gallezot, A. Auroux, *J. Phys. Chem.* **1985**, *89*, 4778-4788.
- [13] a) A. Vjunov, M. A. Derewinski, J. L. Fulton, D. M. Camaioni, J. A. Lercher, *J. Am. Chem. Soc.* **2015**, *137*, 10374-10382; b) J. Brus, L. Kobera, W. Schoefberger, M. Urbanová, P. Klein, P. Sazama, E. Tabor, S. Sklenak, A. V. Fishchuk, J. Dědeček, *Angew. Chem. Int. Ed.* **2015**, *54*, 541-545.
- [14] E. Bourgeat-Lami, P. Massiani, F. Di Renzo, P. Espiau, F. Fajula, T. Des Courières, *Appl. Catal.* **1991**, *72*, 139-152.
- [15] M. Ravi, V. L. Sushkevich, J. A. van Bokhoven, *J. Phys. Chem. C* **2019**, *123*, 15139-15144.
- [16] a) J. A. van Bokhoven, D. C. Koningsberger, P. Kunkeler, H. van Bekkum, A. P. M. Kentgens, *J. Am. Chem. Soc.* **2000**, *122*, 12842-12847; b) J. A. van Bokhoven, A. M. J. van der Eerden, D. C. Koningsberger, *J. Am. Chem. Soc.* **2003**, *125*, 7435-7442.
- [17] a) Z. Yu, S. Li, Q. Wang, A. Zheng, X. Jun, L. Chen, F. Deng, *J. Phys. Chem. C* **2011**, *115*, 22320-22327; b) Z. W. Yu, A. M. Zheng, Q. A. Wang, L. Chen, J. Xu, J. P. Amoureux, F. Deng, *Angew. Chem. Int. Ed.* **2010**, *49*, 8657-8661.
- [18] S. van Donk, J. H. Bitter, A. Verberckmoes, M. Versluijs-Helder, A. Broersma, K. P. de Jong, *Angew. Chem. Int. Ed.* **2005**, *44*, 1360-1363.
- [19] J. Dědeček, B. Wichterlová, *J. Phys. Chem. B* **1999**, *103*, 1462-1476.
- [20] V. Pashkova, S. Sklenak, P. Klein, M. Urbanova, J. Dědeček, *Chem. Eur. J.* **2016**, *22*, 3937-3941.
- [21] B. H. Wouters, T. H. Chen, P. J. Grobet, *J. Am. Chem. Soc.* **1998**, *120*, 11419-11425.
- [22] M. Jeffroy, C. Nieto-Draghi, A. Boutin, *Chem. Mater.* **2017**, *29*, 513-523.
- [23] a) A. A. C. Reule, J. A. Sawada, N. Semagina, *J. Catal.* **2017**, *349*, 98-109; b) P. Bodart, J. B. Nagy, G. Debras, Z. Gabelica, P. A. Jacobs, *J. Phys. Chem.* **1986**, *90*, 5183-5190.
- [24] Y. C. Zhi, H. Shi, L. Y. Mu, Y. Liu, D. H. Mei, D. M. Camaioni, J. A. Lercher, *J. Am. Chem. Soc.* **2015**, *137*, 15781-15794.
- [25] J. Pastvova, D. Kaucky, J. Moravkova, J. Rathousky, S. Sklenak, M. Vorokhta, L. Brabec, R. Pilar, I. Jakubec, E. Tabor, P. Klein, P. Sazama, *ACS Catal.* **2017**, *7*, 5781-5795.
- [26] a) E. S. Zhan, Z. P. Xiong, W. J. Shen, *J. Energy Chem.* **2019**, *36*, 51-63; b) M. Boronat, C. Martinez, A. Corma, *Phys. Chem. Chem. Phys.* **2011**, *13*, 2603-2612.
- [27] a) K. Iyoki, K. Kikumasa, T. Onishi, Y. Yonezawa, A. Chokkalingam, Y. Yanaba, T. Matsumoto, R. Osuga, S. P. Elangovan, J. N. Kondo, A. Endo, T. Okubo, T. Wakihara, *J. Am. Chem. Soc.* **2020**, *142*, 3931-3938; b) S. Proding, M. A. Derewinski, A. Vjunov, S. D. Burton, I. Arslan, J. A. Lercher, *J. Am. Chem. Soc.* **2016**, *138*, 4408-4415.
- [28] K. P. Cao, D. Fan, L. Y. Li, B. H. Fan, L. Y. Wang, D. L. Zhu, Q. Y. Wang, P. Tian, Z. M. Liu, *ACS Catal.* **2020**, *10*, 3372-3380.
- [29] a) Y. A. Zhang, H. J. Han, M. Zhang, H. Y. Wang, Y. G. Chen, C. X. Zhai, J. Sun, J. T. Deng, H. Song, C. L. Zhang, *J. Solid State Chem.* **2021**, *297*, 122035; b) V. G. Gaikar, T. K. Mandal, R. G. Kulkarni, *Sep. Sci. Technol.* **1996**, *31*, 259-270; c) M. Liu, T. Yokoi, M. Yoshioka, H. Imai, J. N. Kondo, T. Tatsumi, *Phys. Chem. Chem. Phys.* **2014**, *16*, 4155-4164.
- [30] a) J. Liu, H. Xue, X. Huang, P.-H. Wu, S.-J. Huang, S.-B. Liu, W. Shen, *Chin. J. Catal.* **2010**, *31*, 729-738; b) Y. Li, Q. Sun, S. Y. Huang, Z. Z. Cheng, K. Cai, J. Lv, X. B. Ma, *Catal. Today* **2018**, *311*, 81-88; c) N. Zhao, Y. Tian, L. F. Zhang, Q. P. Cheng, S. S. Lyu, T. Ding, Z. P. Hu, X. B. Ma, X. G. Li, *Chin. J. Catal.* **2019**, *40*, 895-904.

RESEARCH ARTICLE

Entry for the Table of Contents



When the protonic zeolite mordenite adsorbs pyridine, the nonframework aluminum species, preferentially located in the side pockets, can be forced back into the zeolite framework. This change increases the number of available active sites and enhances the diffusion of dimethyl ether (DME), hence improving the catalytic performances on the DME carbonylation reaction.